ISSN 0016-8521, Geotectonics, 2017, Vol. 51, No. 1, pp. 74–88. © Pleiades Publishing, Inc., 2017.
Original Russian Text © S.Yu. Sokolov, 2017, published in Geotektonika, 2017, No. 1, pp. 81–96.

Sedimentary Cover Deformations in the Equatorial Atlantic and Their Comparison with Geophysical Fields

S. Yu. Sokolov*

Geological Institute, Russian Academy of Sciences, Moscow, 119017 Russia
**e-mail: sysokolov@yandex.ru*

Received June 6, 2016

Abstract—The deformations of the sedimentary cover at near-latitudinal geotraverses west and east of the Mid-Atlantic Ridge in the equatorial part of ocean are compared with potential fields and variations of the V_p/V_s attribute at a depth of ~470 km. The features of sedimentary cover deformations in abyssal basins are formulated, as well as their differences from the undisturbed bedding of sediments. The elements of chain of phenomena with common spatial manifestations and cause-and-effect relationships have been established, including heterogeneous horizontal movements, which make up macrojointing above "cold" mantle blocks at a depth of ~470 km; serpentinization of upper-mantle rocks; the formation of superposed magnetic anomalies; the release of the fluids, which acoustically bleach out the sedimentary sequence in seismic imaging; and decompaction of rocks leading to vertical motions and forced folding. The origin of the Atlantic marginal dislocation zone is explained. The coincidence of the deformation boundary in the equatorial Atlantic with the zero contour line of the V_p/V_s attribute is revealed. This coincidence is an indicator of the rheological state of the upper mantle.

Keywords: equatorial Atlantic, cold mantle block, potential field, sedimentary cover deformation, seismic section, acoustic bleaching

DOI: 10.1134/S0016852117010071

INTRODUCTION

In contrast to remote satellite observations, geophysical data obtained during route and areal measurements aboard research vessels are distinguished by nonuniform density. The zone of the Atlantic between the equator and 25° N is almost a blank spot on map compared to other areas in terms of expeditionary research (Fig. 1). The Geological Institute of the Russian Academy of Sciences (GIN RAS) has carried out a cycle of expeditions on board the R/V *Akademik Nikolai Strakhov* (1985–2006). The data obtained confer an advantage to GIN RAS in studying this deepwater area and contribute substantially to new ideas of ocean tectonics. Academician Yu.M. Pushcharovsky was the scientific supervisor of many expeditions. Data on sedimentary cover deformation obtained by GIN RAS during these expeditions indicate the need to upgrade the model that reproduces tectonic evolution in abyssal parts of the ocean.

Since the early 1970s, in connection with the appearance of new data containing records of withinplate sedimentary cover deformations, this phenomenon has become a matter of discussion, despite the fact that it had been acknowledge earlier only for the initial rift stage of ocean formation [32]. Publications [38, 41] were among the first descriptions of withinplate deformations in Atlantic basins. In particular, the structure of the frontal part of the Barbados accretionary sedimentary wedge has been described in [41]. It has been noted that passive segments of transform faults are traced far to the west beneath the accretionary complex. It is emphasized that the simplified subduction model with deformation at the front of the sedimentary prism is not applicable to interpreting ation the deformations observed in this region. The spatial configuration of deformations is controlled by the previously existing structure of the basement at the passive parts of transforms.

Works carried out along the Transatlantic Angola–Brazil geotraverse (ABGT) at a latitude of 12° S in a tract 500–1000 km wide and ~4400 km in extent from the Brazil Basin to the Angola Basin are especially noteworthy. These works were performed by the Ministry of Geology and the USSR Academy of Sciences (more than 20 legs). In scale and minuteness, this traverse has no analogs in world practice. It is based on a deep seismic sounding (DSS) profile and the correlation method of refracted waves (CMRW), which made it possible to construct a section of the lithosphere to a depth of 80 km. In addition, the survey was accompanied by a standard complex of route geophysical measurements, including continuous seismic profiling (CSP). The western and eastern segments of geotraverse are charac-

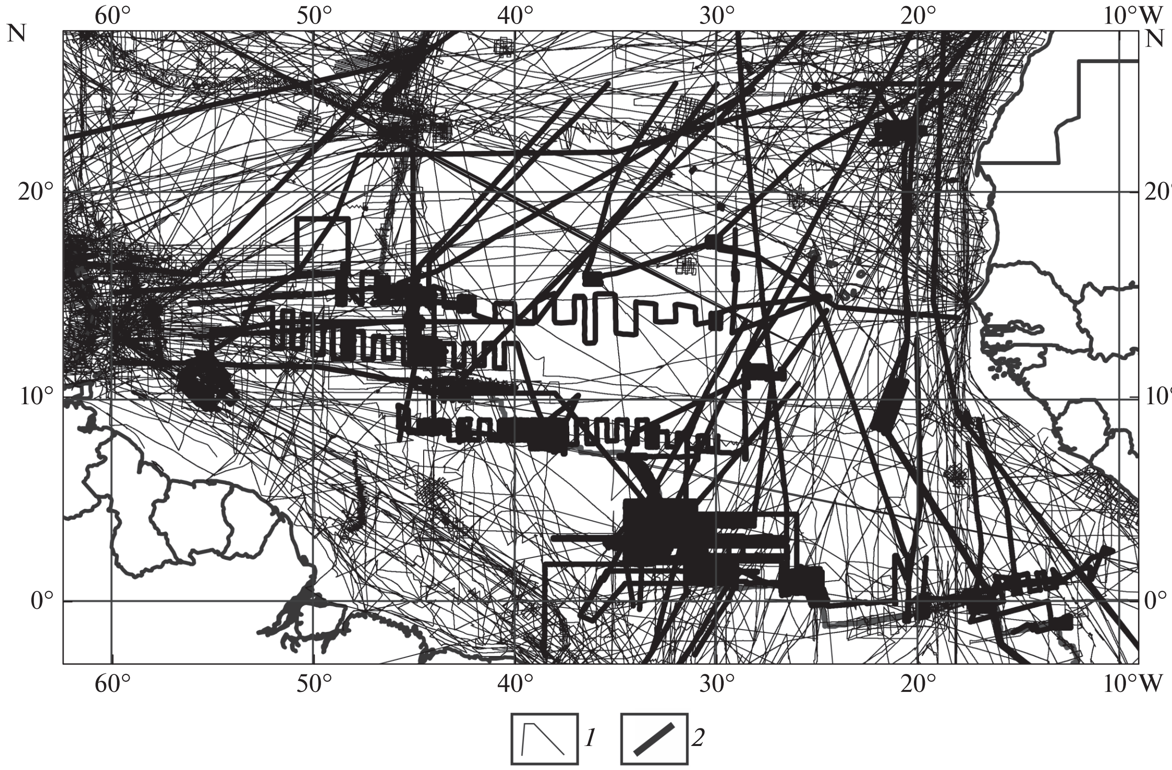

Fig. 1. Coverage of equatorial Atlantic by areal and route geophysical measurements based on open access data (*1*) [44] and (*2*) data from the Geological Institute, Russian Academy of Sciences (GIN RAS) collected aboard the R/V *Akademik Nikolai Strakhov*.

terized by sedimentary cover deformations, which were established by seismic surveying in 1984.

Deformation phenomena were repeatedly noted in Atlantic by expeditions of the RAS Institute of Oceanology along with a study of classic within-plate deformation zones in the Indian Ocean. A review of the sedimentary cover structure at the bottom of basins obtained on the 31st cruise of R/V *Dmitry Mendeleev* (1983–1984) has been published [8]. The late Miocene plicated sedimentary cover deformations revealed in the trough of eastern passive segment of the Cape Verde Fault [8] are overlapped by younger sediments with an angular unconformity. Piercement structures in Atlantic basins were repeatedly reported by expeditions of the RAS Institute of Oceanology under the supervision of Yu.P. Neprochnov and L.R. Merklin [16].

The data obtained on the second [1] and the third cruises of the R/V *Akademik Nikolai Strakhov* of GIN RAS provided evidence for sedimentary cover deformation in Atlantic basins over a vast within-plate space. In general, the sedimentary cover is a seismic sequence that fills the dissected topography of the magmatic basement. Differentiated vertical tectonic movements initiated the tilting of sedimentary bodies, numerous episodes of acoustic bleaching of sedimentary cover in the deformed areas, and zones of deformation along the eastern passive segment of 15°20' (Cape Verde) Fault. A series of works published by the Laboratory of Geomorphology and Tectonics of the Oceanic Bottom, GIN RAS [10–12, 33], integrates the results obtained on several cruises of the R/V *Akademik Nikolai Strakhov* in the equatorial segment of the Atlantic Ocean. The multiple reactivation of tectonic processes was revealed not only in the axial zone, but also far beyond its limits (more than 500 km away), as well as asymmetry relative to the MAR.

Comparison of satellite altimetry data with materials from multibeam sonars and continuous seismic profiling obtained by GIN RAS on board the R/V *Akademik Nikolai Strakhov* made possible to draw important conclusions on the structure of the passive parts of transform faults and sedimentary cover deformation [13]. Complex deformations related to vertical positive movements of oceanic crustal blocks beyond the limits of the spreading zone have been established. The general configuration of shear zones in sediments and the character of dislocations make it possible to assume that within-plate deformations at a great distance from the MAR may have been caused by strike-slip kinematics, including along passive segments of fault-line troughs [13]. For another well-known zone of within-plate deformations in the northeastern part of the Indian Ocean, it had been inferred that theor origin is a result of strike-slip offset along NE-trending faults, which do not coincide with passive segments of transform faults.

Investigations of the Geological Institute on board the R/V *Akademik Nikolai Strakhov* supervised by Yu.M. Pushcharovsky since 1985 are the first attempts to record such a phenomenon as within-plate sedimentary cover deformations in Atlantic basins unrelated to plate boundaries or continental margins. Many available seismic data and their discussion in publications have revealed a discrepancy between factual data and the geodynamic model of plate tectonics, which gives a new interpretation of basic tectonic structures but does not take into account the lack of rigid within-plate space. Nevertheless, precisely this property has been established as a necessary condition for the observed deformations. Since the latter are matter of debate, it is believed that further research of their spatial distribution and comparison with geophysical fields would be helpful.

MAIN ATTRIBUTES OF DEFORMATIONS

The following attributes are used as criteria for revealing deformational structures in abyssal basins.

(1) The occurrence of extended and contrasting reflectors inclined at angle of $>1°$ in the seismoacoustic imaging of the sedimentary sequence (Fig. 2, feature 1). Reflectors with a dip angle of $< 1°$ can be formed by envelopment, because this slope is critical for unconsolidated sediments. When this angle is exceed, unconsolidated sediment starts to flow along the slope [24]. At angles $>1°$, it is hardly probable that deposition of the sedimentary sequence and its lithification will reach a state with contrasting acoustic properties creating a reflector with inclined boundaries within a cover except for the following cases:

—reflectors immediately overlapping the acoustic basement (significant differential compaction);

—undulatory images formed by intense discharge of gravitational flow (turbidites) and contour flows (drifts) with lateral progradation.

(2) Folds of constant thickness between wavy curved reflectors (Fig. 2, feature 2). An exception is a slope $<1°$, when a heterogeneous basement is enveloped by unconsolidated sediments that retain the shape.

(3) Disjunctive disturbance with displacement of reflector phases or with vertical zones of loss of coherence (Fig. 2, feature 3). An exception is vertical acoustic bleaching related to fluid flow.

(4) Piercement structures (injective disturbances) defined by a reduced thickness of sediments above the unit of growth onset and/or local erosion of this unit and gradual flattening of the overlying sequence after growth ceases (Fig. 2, feature 4).

(5) A structural unconformity in the form of a near-horizontal overlap of young sediments over older ones with signs of folding, disjunctive disturbance, and growth structures occasionally accompanied by erosion (Fig. 2, sign 5).

(6) Acoustic bleaching of abyssal sections associated with delivery of fluids in the slightly consolidated cover takes place near inliers of the acoustic basement, which are markedly higher than the level of the bottom (Fig. 2, sign 6). The bleached rock bodies are represented either by vertical pipes or nearly horizontal lenses localized immediately above the basement. Acoustic bleaching accompanies the most deformational basement structures.

These attributes make it possible to determine the sedimentary cover deformation. Further, it is suggested that certain descriptions of deformation occur in seismic records.

As noted in [15], a zone of marginal dislocations (ZMD) up to 400 km in width and accompanied by deformation of sediments has been fully contoured in the Atlantic Ocean since the first works of G.B. Udintsev published in 1966. The cause of deformation is thought to be lateral compression, although the configuration of the deformed reflectors recorded in many routes does not correspond to the features characteristic of compression.

The integration of latitudinal geotraverses carried out using continuous seismic profiling (CSP) on the second cruise of the R/V *Akademik Nikolai Strakhov* is given in [1]. The area between 11° and 20° N 200–400 km in width at the western flank of the MAR coincides with the ZMD after [15]. Plicative and disjunctive deformations of the sedimentary cover related to vertical motions of basement blocks developed in this area. In the sedimentary sequence between the bottom and the acoustic basement formed by an undulatory field diffracted from the surface imperfections of basalts, three seismic complexes are distinguished. All of them are disturbed in deformation zones. This allows the idea that the disturbances are of contemporary age. It has also been noted that in some cases, only complexes 2 and 3 have been disturbed, whereas the youngest complex 1 overlies them, filling the roughness of roof topography related to older complexes and the acoustic basement.

ABGT research revealed numerous manifestations of within-plate deformations with features of latitudinal compression. Pilipenko [17–19] describes them together with classic deformations in the northeastern Indian Ocean. In the western Brazil Basin, presedimentation thrust faults with eastern vergence are observed in near-latitudinal sections. In the eastern part of the basin 600–100 km from the MAR (the age of the crust is 5–7 Ma), thrust faults have been revealed. They offset the sedimentary section with an amplitude of reverse faulting up to 150 m. It is noteworthy that imbricate thrust structures with eastern vergence are also known in the Angola Basin.

The dimensions of blocks between disturbances vary from 7 to 15 km. Structural inhomogeneities with

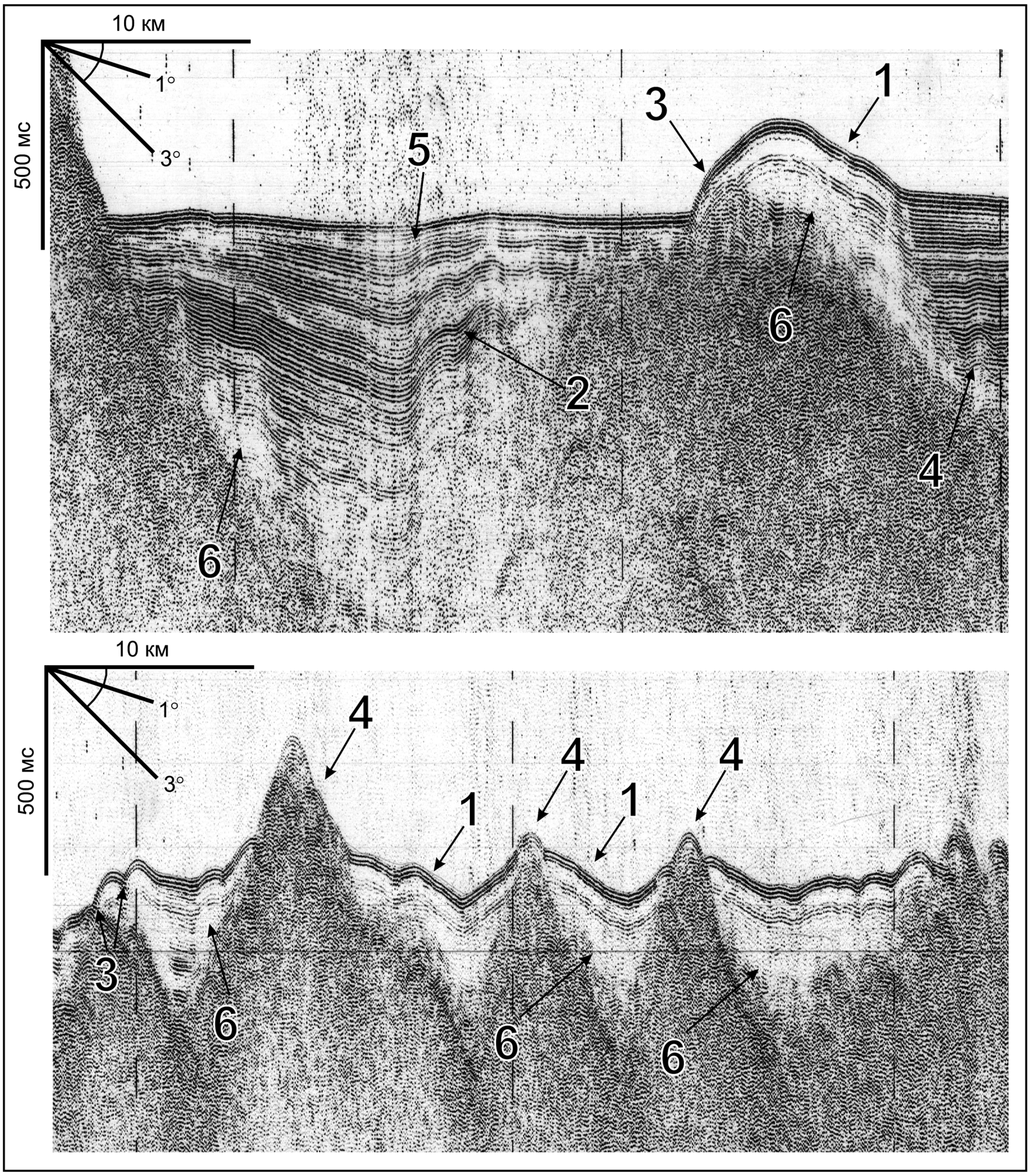

Fig. 2. Evidence for sedimentary cover deformations in abyssal basins based on data obtained on expeditions by GIN RAS (numerals in figure): 1, reflectors in sedimentary sequence inclined at angle of > 1°; 2, constant thickness between folded-type reflectors in record ; 3, fault; 4, piercement structure; 5, structural unconformity; 6, acoustic bleaching of sedimentary sequence in form of lenses and gas pipes.

oblique northwestern orientation have been noted west of the MAR. Pilipenko [21] interprets the origin of these structures in terms of nonlinear geodynamics Pushcharovsky and tectonic delamination.

Along the divergent plate–MAR boundary at a distance of up to 350 km from the rift axis, when the lithosphere has cooled and the upper mantle is serpentinized at the flanks of the MAR [31], deformations of thin sedimentary layers are mainly expressed in low-amplitude normal faults and inclined reflectors in sedimentary bodies filling isolated niches in the basement [33]. These deformations are inscribed into the working geodynamic model of oceanic lithosphere formation. The anomalous structure of the sedimentary cover in the frontal part of the Barbados accretionary wedge should also be referred to the deformations inscribed into this model; however, forced folds that appear at the transition to the troughs filled with sediments are poorly explainable in terms of interaction with the front of the prism. Deformations of the oceanic crust bearing seismic features of fault plane flattening are described in [23]. Tectonic delamination of the oceanic crust is formed in this way. The overwhelming majority of examples given in [23] are localized near plate boundaries close to large transform faults. This implies that these deformations are not related to the within-plate deformations proper and can be explained by interaction (transpression or transtension) of plates along the boundaries between them, which wanes away from these boundaries.

Raznitsin [22] emphasizes that zones of tectonic hummocking and stacking occupy no less than 70% of the area in the deepwater part of the Brazil Basin. Here, the southwestern slopes of folds are distinctly steeper than their northeastern counterparts. In the basins, thrust faults symmetrically verge toward the MAR, although in the Angola Basin, an eastward vergence appears as well. In general, Raznitsin and Pilipenko [22] distinguish both a leveled and dissected (close to the MAR axis) topography of the basement roof in the near-latitudinal compression setting. It is pointed that compression can occur in the form of thrust faults along those detachments, along which listric normal faults that formed in the course of rifting during the extension phase. The cause of delamination is not discussed here.

One more phenomenon important for comprehending deformational processes in transform strike-slip transform fault zones [40] should be noted. As was shown by the example of the doubled Charlie Gibbs Fault Zone, synthetic Riedel shears exist a few tens of kilometers from the main fault at the flanks of the MAR adjoining the offset part of a transform fault and are traced in the near-latitudinal direction beyond its limits near the passive part of the fault. This was concluded based on data obtained by a GLORIA deepwater sonar system (United Kingdom). The occurrence of structures oblique in orientation relative to the main orthogonal elements of spreading tectogenesis has been quite well substantiated by stress distribution in a shear setting. Similar oblique troughs in the equatorial Atlantic are filled with sedimentary cover [31]. The sedimentary cover in the offset parts of transform faults [40] is deformed by shear. A more mobile limb in the transverse seismic section of unconsolidated sediments has been lifted up to 200 m.

COMPARISON WITH THE DEEP GEODYNAMIC STATE

The ratio of shear and compressional velocities is an important parameter that determines the deep geodynamic state of the upper mantle. This ratio depends on the Poisson coefficient [27] and determines the ability of a medium to flow (rheology). In exploration geophysics, the attributes that take this ratio into account are used to detect anomalies in an undulatory field related to fluids [6]. Comparison of geological–geophysical parameters along the MAR axis with the $\delta(Vp/Vs)$ attribute [26] has shown that they are related to alternating minima and maxima of the attribute at a depth of ~500 km. The minima of an attribute are related to macrojointing at the surface, large (>200 km) near-latitudinal offsets of the MAR axis, atypical mechanisms of earthquake sources, and minimum asymmetry of the half-rate of spreading. Since the half-rates of spreading can differ by factor of several between blocks separated by transform faults, deformation between blocks along the passive parts of these faults is possible. The maxima of the $\delta(Vp/Vs)$ attribute are related to long segments of the MAR devoid of transform faults and with minimum Bouguer anomalies pointing to regional decompaction and heating. The aforementioned parameters and their features show that the geodynamic state of the mantle at a depth of ~500 km or more determines the distribution of these parameters at the surface.

Figure 3 shows horizontal section of the $\delta(V_p/V_s)$ attribute cube calculated from seismic tomography data for P and S waves for the equatorial segment of the Atlantic at a depth of 470 km. "Cold" blocks (values <0) are beneath zones with the longest transform displacements of the MAR axis, and "hot" zones (values >0) are in areas of local offsets of the African superplume: the Azores, Canary, and Cape Verde islands. The difference in rheologic properties at the above-mentioned depth ensures a more mobile dynamics of hot zones in ductile mantle and occurrence of elevated macrojointing in brittle mantle with atypical seismicity in zones of great the MAR offsets above hot blocks. The map in Fig. 3 shows that a continuous hot system is lacking beneath the MAR and that the background value in Atlantic is mainly cold. The general configuration of the anomalous field contains a group of isolated hot maxima built into the background field and corresponding to the aforementioned superplume offsets.

The works performed by GIN RAS in the equatorial segment of the MAR (Fig. 1) show that within-plate sedimentary cover deformations are localized in a cold block at a depth of ~470 km (Fig. 3). The established deformations are also related to the passive parts of transform faults [13] and NW-trending faults [14], which are oriented at the same azimuth as the cold mantle block. To analyze the spatial distribution of deformations and their relationships with geophysical fields, it is expedient to select long, straight geotraverses that crosscut anomalous zones at a right angle to the MAR axis on both flanks (Fig. 3).

GEOTRAVERSE OF THE WESTERN FLANK OF THE MAR

Figure 4 shows the geotraverse of the western flank of the MAR, where the sedimentary cover is traced from the minimum thickness in the east at the flanks of the MAR to 1.0–1.3 km in the west, in the foredeep of the Barbados accretionary prism at the limiting

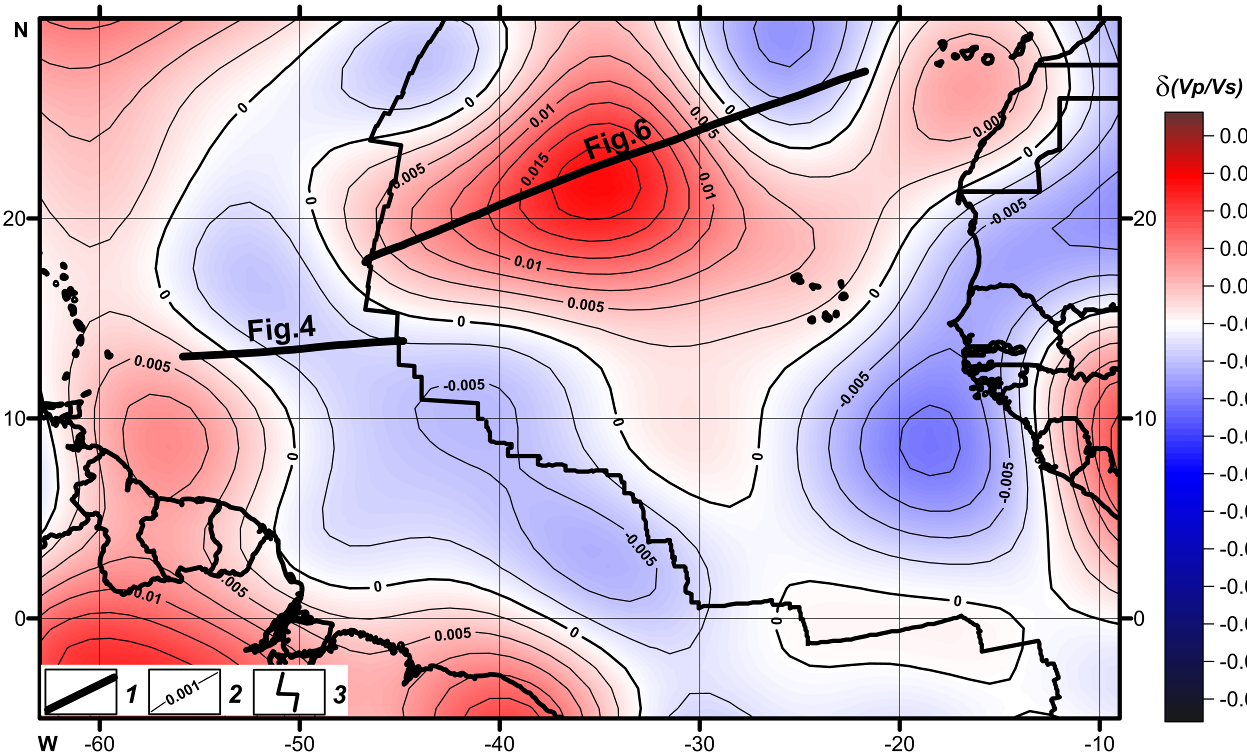

Fig. 3. Horizontal section of variation cube of $\delta(V_p/V_s)$ ratio calculated from seismic tomography data for P and S waves [29, 34, 42] at depth of 470 km. (*1*) Position of sections along continuous seismic profiles (CSP) and graphs of potential fields presented in figures with corresponding numbers; (*2*) contour lines of $\delta(V_p/V_s)$ ratio; (*3*) axial line of MAR.

depth inherent to the CSP method. The section exhibits sedimentary cover deformations (Fig. 5) and acoustic bleaching of the lower part of the section adjoining the acoustic basement. Note first that in the midst of a fragment near the longitudinal mark of –51° W (Fig. 5), an almost undeformed attitude of reflectors is observed: the record of sedimentary pockets is typical abyssal seismofacies of filling with subsequent differential compaction that resulted in subsidence of initially horizontal reflectors in the deeps of the basement and relative uplift on slopes. The asperities of reflectors flatten toward the present-day sedimentation surface. The main feature of such sedimentary bodies is their overlapping of the basement and lack of enveloping reflectors. Nevertheless, the separate piercement structures occur in this fragment of the standard abyssal record.

The deformation origin of reflectors in the sedimentary cover on a rise near –50° W (Fig. 5) is substantiated by the fact that main reflectors envelop the basement; their thickness reaches 300 ms, and the real dip angles are ~2°, occasionally up to 4°. The accumulation of clayey sediments of such thickness in abyssess and at such angles with the formation of intermediate reflectors is hardly realistic without slumping. The deformational origin of these structures often casts doubt; however, angular degrees and intermediate reflectors with constant thickness within bends indicate, in our opinion, correspondence with contemporary deformations rather than background sedimentation. The latter can fill surface irregularities, but at angles lower than 1°. With an increase in angles and thickness in the vicinity of the seismic MAR, poorly consolidated sediments tend toward local leveling of the basement roughness.

The origin of acoustic bleaching at the base of the sedimentary cover is explained, almost without any alternative version, by release of fluid from rocks of the acoustic basement. The origin of the fluid itself is a special subject of discussion. The most substantiated is the conjecture that explains appearance of fluids as products of serpentinization with the release of hydrogen and formation of methane [4, 30]. Due to elevated macrojointing and cooling of the lithosphere with distance from the MAR, water becomes accessible to ultramafic rocks of the upper mantle, which are transformed into serpentinites at a temperature of ~100°C to ~450°C. Methane formed as a product of interaction of H_2 and CO_2 creates acoustic anomalies in the seismic record. Especially strong bleaching has been noted within –53.5° to –52° W (Fig. 5). Bleaching primarily involves the entire interval from basement to seafloor, but in the sedimentary pocket at –52° W this process affects only the lower part of the cover, which is equal in thickness to other bleaching episodes (~250 ms). If the rate of saturation of the sedimentary sequence with fluid is taken as constant, it can be suggested that its release began simultaneously

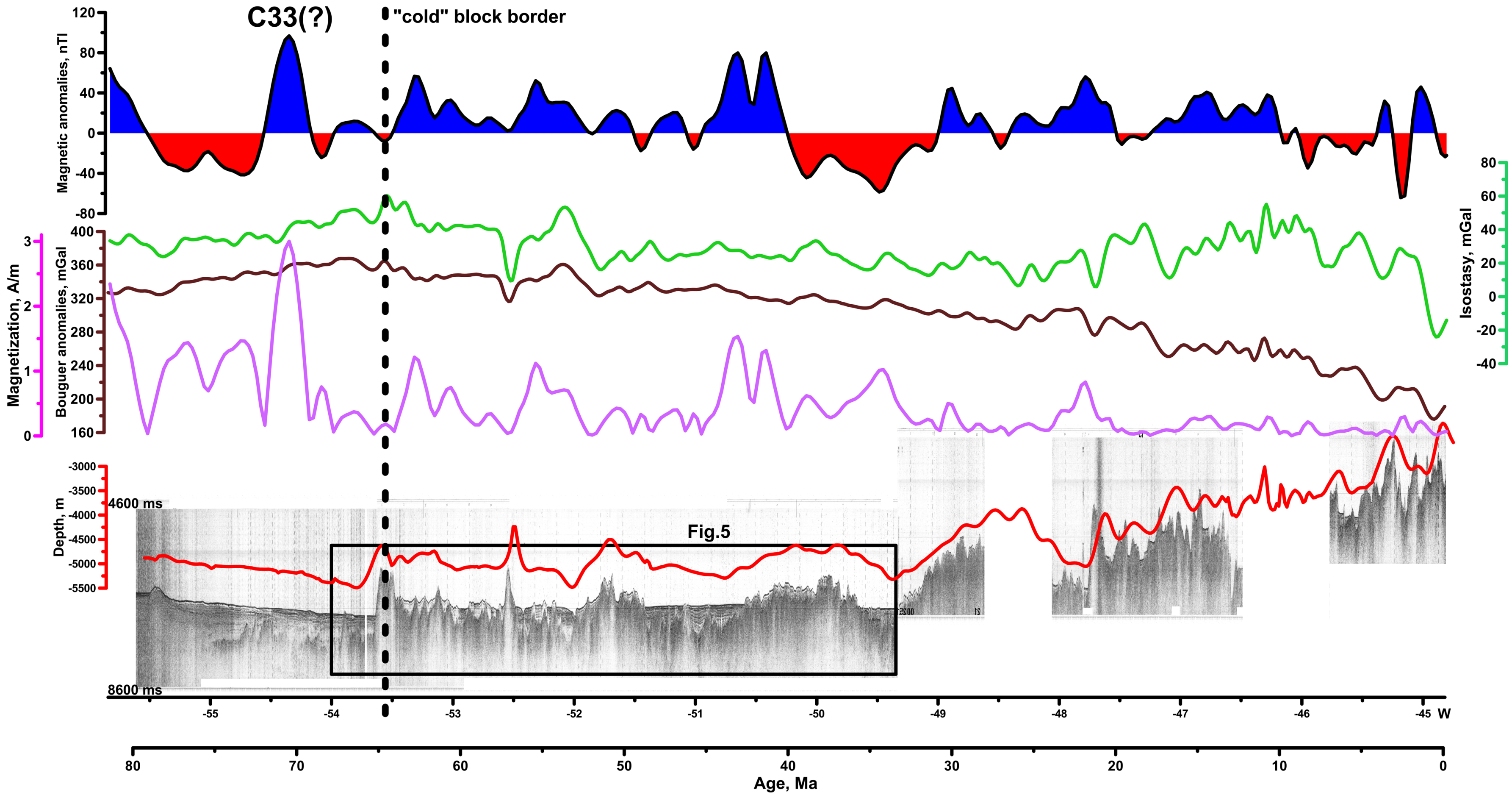

Fig. 4. Geotraverse of western flank of MAR: section along CSP from frontal Barbados accretionary prism (13°7′ N, 55°53′ W) to MAR (13°51′ N, 44°48′ W) in abyssal Demerara Basin, see Fig. 3 for location; ninth cruise of R/V *Akademik Nikolai Strakhov* (GIN RAS, 1989; Yu.N. Raznitsin, head of cruise; Poberzhin V.M., head of CSP group). Graphs of potential fields (from bottom to top): topography, m [43]; magnetization of basement, A/m; Bouguer anomalies, mGal; anomalous magnetic field, nT [36]. Total geotraverse length is 1230 km. Age scale is given after [37].

throughout the profile and most likely synchronously with deformation. A gas pipe as a vertical band of acoustic bleaching constant in width occurs near the piercement structure in the central part of the pocket at –51° W (Fig. 5). The reduced thickness between reflectors in the upper part of the section, in contrast to the constant thickness between the reflectors formed earlier, marks the onset of piercement structure formation. The combination of piercement structures and the acoustic bleaching record is an indicator of deformation.

Deformed sediments, except for piercement structures, are observed at juts of the acoustic basement situated hypsometrically 300–500 m higher on average than the bottom of basins (Figs. 4, 5). The rocks occurring on these juts resemble envelopments in shape, but are actually not in terms of sedimentary cover formation. Similar surface imperfections of the surface of the basaltic basement below this level are filled with sediments without the formation of inclined reflectors that envelopthe basement.

The folding of lateral bending (forced folding) is why the deformed sediments that occur at juts of the basement do not rise above the carbonate compensation level. Folding occurred owing to an increase in the volume of rock subject to serpentinization and to vertical movements under conditions of a less viscous state of rocks. The cause-and-effect relationship between deformation zones and the development of serpentinized rocks has been established and repeatedly described in literature on the Indian Ocean, e.g., [5, 9]. It is noteworthy that the western boundary of the deformed zone (Fig. 4) coincides with the boundary of the cold mantle block according to data on the V_p/V_s ratio (Fig. 3), which is related to the zones of maximum displacement of the MAR and macrojointing. The latter is a necessary element for access of water to upper-mantle rocks and the onset of serpentinization.

The topographic profile shown in Fig. 4 is based on a small-scale 30-s GEBCO matrix [43] for the general structural background if gaps in seismic record are present. Then, from bottom to top, the graph of magnetization calculated from data on the anomalous magnetic field (AMP) EMAG2 [36] (upper graph) follows, using information on the topography and thickness of the sedimentary cover as the total distance to the source of the field. The regions of deformations and acoustic bleaching of the base of the section are represented by appreciable magnetization anomalies, which are higher in amplitude than anomalies close to the MAR. Because the conditions for serpentinization of mantle ultramafic rocks are created as the lithosphere cools at the flanks, the formation of magnetoactive interlayers is activated and this results in the appearance of a supplementary AMP component, which disturbs the system of anomalies formed by spreading. This indicator is important for interpreting

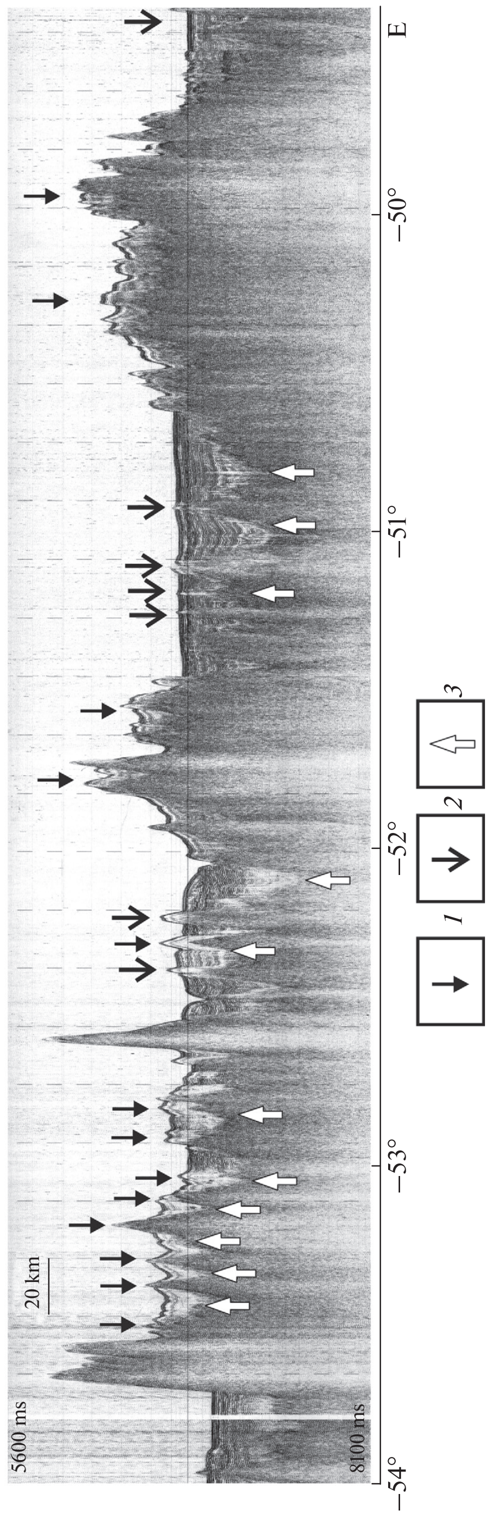

Fig. 5. Geotraverse fragment of western flank of MAR (see Fig. 3 for location) with sedimentary cover deformations. Ninth cruise of R/V *Akademik Nikolai Strakhov* (GIN RAS, 1989; Yu.N. Raznitsin, head of cruise; Poberzhin V.M., head of CSP group). (*1*) Forced fold center; (*2*) piercement structure, (*3*) zone of acoustic bleaching.

deformations, because it indicates the source of serpentinization, where the rock volume increases up to 20% and the rock density correspondingly decreases [27]. The formation of magnetite as a by-product [4] is no less important. Due to this process, the AMP intensity increases with distance from the MAR [3]. Strong anomaly C33 in the west of the geotraverse (Fig. 4) is noteworthy. The first Cenozoic linear anomalies C34 and 33 are characterized by a high amplitude throughout Atlantic [36] and are most likely not related to secondary processes of magnetoactive layer formation.

The decrease in density of serpentinized rocks along with their quite large volume gives rise to extensive minimum Bouguer anomalies (Fig. 4). At a longitude of –52.5° W, the appreciable minimum is 25 mGal lower than the adjacent background value in the basin (~350 mGal). At a longitude of –51.75° W, a shallower minimum is noted, but both are related to deformational zones. These relationships make it possible to estimate the thickness of serpentinized rocks on the basis of the gravity field; however, for now, the statistics for deformed zones are insufficient to construct a model. The level of Bouguer anomalies calculated without thermal correction regularly decreases toward the MAR axis, where the gravitational effect of the heated and decompacted upper mantle matter is prevalent.

The calculation of isostatic anomalies determines the gravitational effect of the mantle surface calculated from the bottom topography in proportion to the density ratio (Airy model), which is subtracted from the Bouguer anomalies calculated for the same topography [25]. The consideration of Bouguer and isostatic anomalies for these geotraverses (Fig. 4) shows that a positive correlation of these fields calculated from the same data is established in abyssal basins devoid of disturbed isostatic equilibrium comparable to that in the MAR. The correlation is violated in the rift zone of the MAR and at its flanks up to 350 km apart. Isostatic equilibrium is disturbed in these zones by rifting and transition from heated to cooled states, which is primarily achieved at the above-mentioned distance. At the same distances (350–400 km), isostatic anomalies decrease (Fig. 4), approaching 20–25 mGal, the background values typical of the Atlantic [2]. The increase in isostatic values west of longitude of –52° W (Fig. 4) is related to contemporary movements with vertical components, which ensure excess mass by a mechanism other than ascent of matter in the rift zone. This increase in mass formed recently, because isostatic compensation up to the background value has not yet taken place. The deformed sediments contain no signs of leveling, but contemporary downcuttings of bottom currents occur near longitudes of –52° and –52.5° W. A similar combination of potential fields is observed at the geotraverse near –47.6° W, but because significant sedimentary cover is not known there, it is hardly possible to learn anything reasonable about the deformation of the surface of the acoustic basement.

GEOTRAVERSE OF THE EASTERN FLANK OF THE MAR

Figure 6 shows the geotraverse of the eastern flank of the MAR. The significant sedimentary cover therein begins from a longitude of –30° W in the passive part of the recluse transform fault with a distinctly expressed trough but without an active part in the the MAR zone where the bottom depth exceeds 6000 m. The cover is observed in the section of the aforementioned trough northeast of the passive part of the Chain Fault (longitude of –34.2° W). The section up to a longitude of –28.3° W is represented by a strainless sedimentary cover, which fills asperities of the acoustic basement. Farther to the northeast the seismic facies of filling gives way to the echeloned system of ten cuesta-like uplifts 10 to 20 km wide overlapped by sedimentary cover with reflectors at angles of 1.5° to 4° (Fig. 7, fragment 1). In addition to deformations, the section contains acoustic bleaching of the lower part of the sedimentary sequence adjoining the acoustic basement and gas pipes (Fig. 7, fragment 2). Note the mosaic pattern of deformation zones with undisturbed intervals between them (–27.9° W), as well as the similarity of deformations (especially the adjoining seamount) with an imbricate system of reverse faults, which can be determined by the morphology of reflectors between the bottom and basement, including intermediate reflectors (Fig. 7, fragment 1). This morphology is typical of reverse–thrust faults. In addition, all they have a southwestern vergence, which is consistent with the orientation of section.

Northeast of seamount, the character of deformation changes. The main part of the sedimentary cover (Fig. 7, fragment 2) is the standard abyssal record with differential compaction of filling facies with separate piercement structures (e.g., near longitudes of –24.5° and –24° W). The acoustic bleaching of the base of the sedimentary cover is a layer above the basement and vertical gas pipes. Especially strong bleaching is observed near a longitude of –25° W, 120 km northeast of the seamount. The overall northeastern part of the profile, except for the indicated interval, is penetrated by gas pipes, which do not reach the roof of the sedimentary cover for 150 to 250 ms irrespective of pipe root depth. This implies that the most likely cause is related to the lithology of sedimentary rocks at this depth. According to the result of DSDP (leg 14, Hole 138 [35]), a sequence of compacted clay presumably Early Cenozoic in age occupies an interval of 150 to 240 m below the seafloor. The drilling rate within this interval was abruptly slowed down four times. Clay with flint and siltstone interbeds in cherty cement lie beneath this sequence. The sedimentary rocks of this interval are most likely a barrier to the advance of gas pipes upsection. The projection of Hole 138 on section

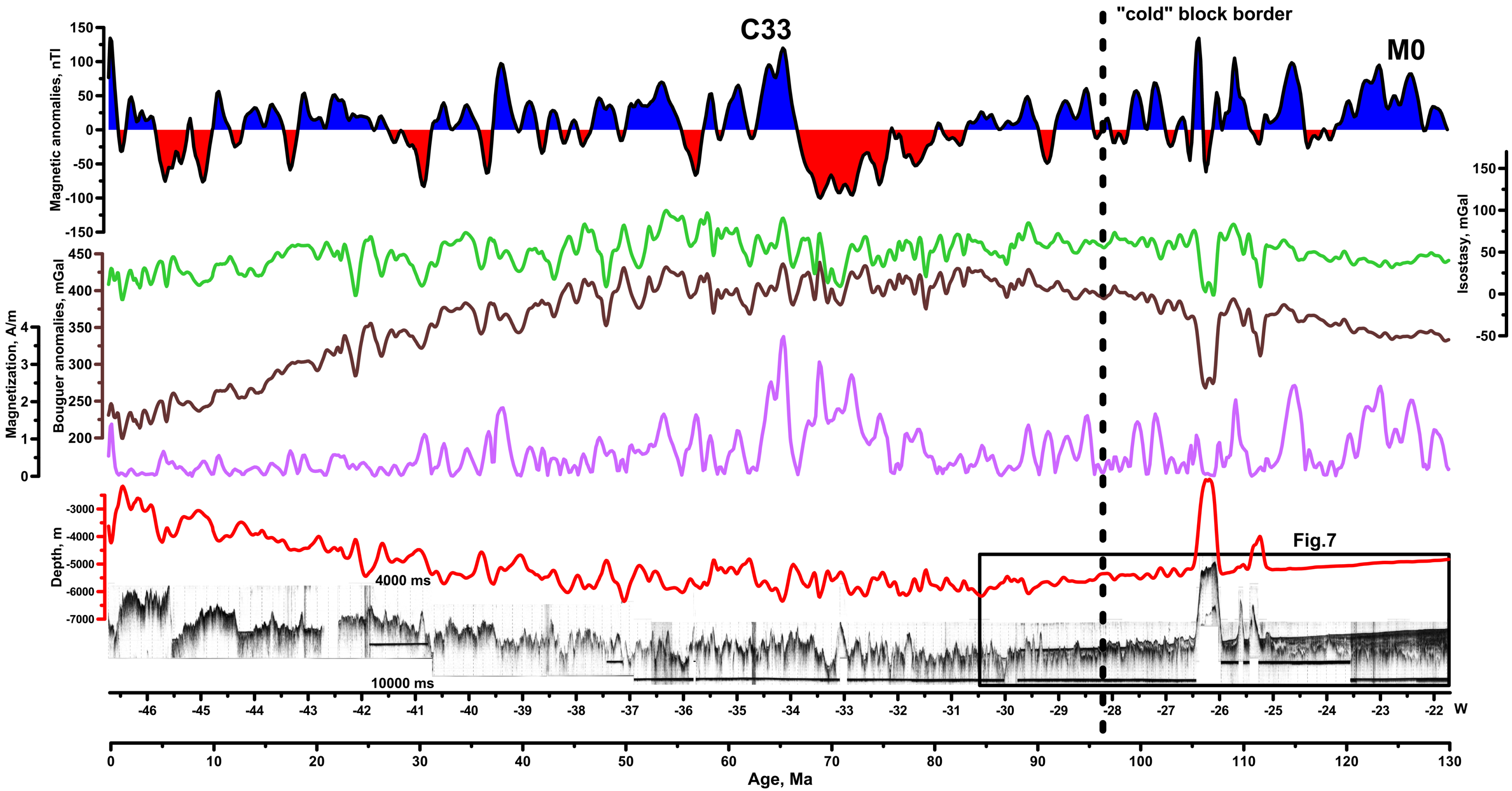

Fig. 6. Geotraverse of eastern flank of MAR: section along CSP from MAR (17°48′ N, 46°43′ W) to Canary Islands (27°21′ N, 21°41′ W) in abyssal Cape Verde Basin (see Fig. 3 for location). Twelfth cruise of R/V *Akademik Boris Petrov* (GEOKhI RAS, 1989; L.V. Dmitriev, head of cruise; V.N. Efimov, head of CSP group). Graphs of potential fields (from bottom to top): topography, m [43]; magnetization of basement, A/m; Bouguer anomalies, mGal; anomalous magnetic field, nT [36]. Total geotraverse length is 3000 km. Age scale is given after [37].

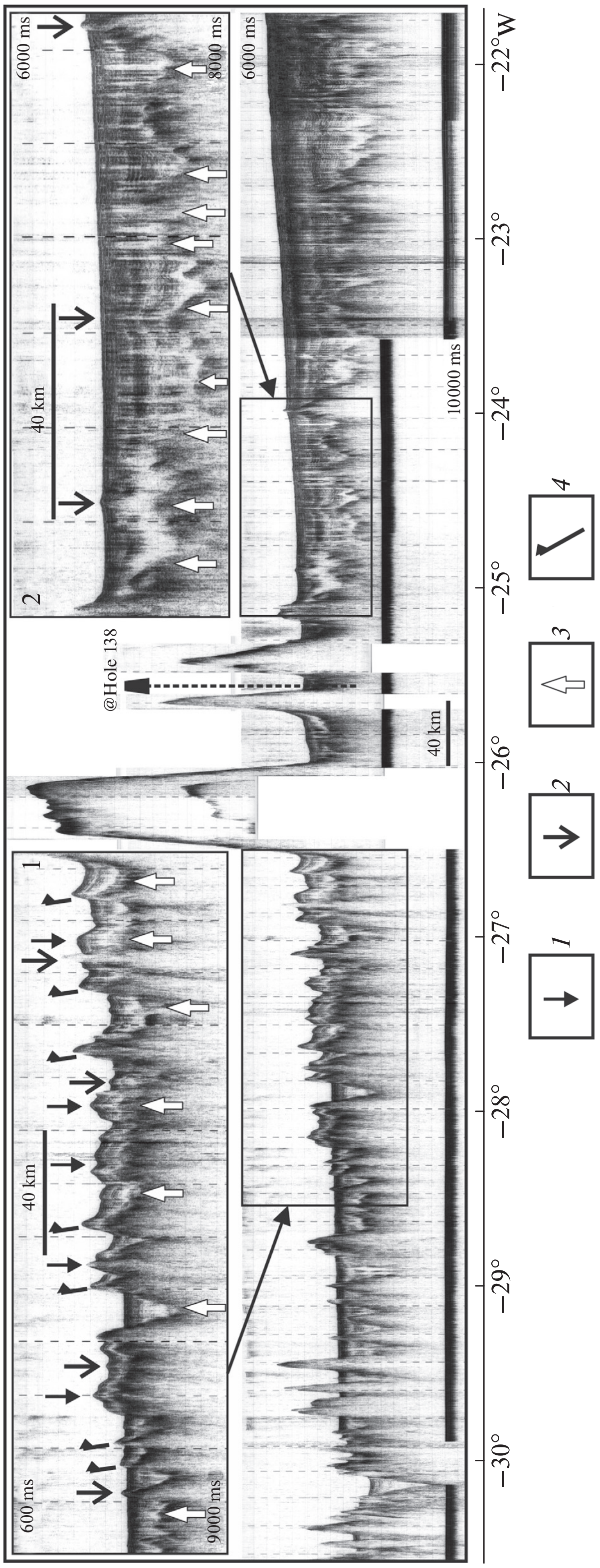

Fig. 7. Geotraverse of fragment east of MAR (see Fig. 3 for location) with sedimentary cover deformations. Twelfth cruise of R/V *Akademik Boris Petrov* (GEOKhI RAS, 1989; L.V. Dmitriev, head of cruise; V.N. Efimov, head of CSP group). Fragment 1 shows deformation west of seamount; fragment 2 is acoustic bleaching of sedimentary sequence east of seamount. DSDP Hole 138 [35] is projected onto section line. (*1*) forced fold center; (*2*) piercement structure, (*3*) zone of acoustic bleaching, (*4*) reverse fault.

is shown in Fig. 7. The proximity of strong bleaching to a longitude of –25° W and volcanic mountains makes the additional magmatic version of origin of the bleaching fluid important. In other parts of the section (Fig. 7), the version based on serpentinization is the main one. The chemical composition of sediments and their lithology remain unknown.

In the eastern geotraverse, as well as in its western counterpart, deformed sediments, except for piercement structures, occur at juts of the acoustic basement situated hypsometrically 300–500 m higher on average than the bottom of basins (Figs. 4–7). As indicated above, deformations occur owing to an increase in the rock volume subject to serpentinization and processes related to the arrival of fluids. It is noteworthy that in the eastern geotraverse, the western boundary of the deformed zone (Fig. 5) also coincides with boundary of the cold mantle block determined by the V_p/V_s ratio at a depth of 470 km (Fig. 3), which is related to macrojointing at the surface. The latter is necessary for access of water to the upper mantle rocks and for initiation of serpentinization.

The topography is shown in Fig. 6 after the GEBCO matrix [43] as the general structural background of the seismic record. The graph of magnetization that follows (from bottom to top), has been calculated from the anomalous magnetic field (AMF) EMAG2 [36] (upper graph) using the data on the topography and thickness of the sedimentary cover as the total distance to the source of the field. The anomalies in region of the last Cenozoic and first Mesozoic chrons have elevated amplitudes throughout the Atlantic and are most likely related to the productivity of magmatism. Magnetization anomalies in the region of deformation and acoustic bleaching at the base of the section are characterized by an elevated level compared to the flanks of the MAR. At higher levels, this was related to cooling of the lithosphere and formation of conditions for the serpentinization of mantle ultramafic rocks with the crystallization of magnetite [4]. The lack of a peak above the seamount is related to the intersection of an intense (up to 250 nT) [36] but asymmetric anomaly of the seamount along the line of transition through zero from maximum to minimum. Just like the above-mentionedhigh AMF values, they are also related to productive but point magmatism.

In the zone of deformations northeast of –30° W, the background level of Bouguer anomalies is reduced (Fig. 6) likely due to a decrease in the density of serpentinized rocks. This effect, however, does not exceed 20–25 mGal and is expressed in small local minima. Manifestations of productive point magmatism (longitude of –26.2° W) result in a local decrease in Bouguer anomalies by more than 110 mGal, but do not create a regional background. The decrease in the background values of Bouguer anomalies at a longitude of –30° W from 400 to 340 mGal is caused by unaccounted-for effect of the sedimentary layer, the thickness of which at the northeastern boundary of the section reaches 2000 ms (Fig. 7). With allowance for the estimated velocity of seismic waves, the thickness of this layer can reach 3.2 km. Taking into account the difference in density between sediments and the basaltic layer, the negative gravitational effect of unaccounted-for masses with an average density of 2.75 g/cm^3 used to calculate Bouguer anomalies will gradually increase with increasing sediment thickness, so that the background level of the anomalous field will be reduced. As in the western geotraverse, the level of Bouguer anomalies calculated without thermal correction regularly decreases toward the MAR axis.

Calculationof isostatic anomalies and their comparison with Bouguer anomalies in the eastern geotraverse (Fig. 6) show that a positive correlation of these fields, beginning with variations 25–30 km in width, has been recorded in abyssal basins where isostatic equilibrium is not disturbed. The correlation is distorted within the interval from the rift zone of the MAR and its flanks for ~450 km, after which the behavior of the fields is synchronized. This deviation from a decrease in Bouguer anomalies has the same width as at the western flank of the MAR; however, isostasy is lower than the background value. Such asymmetry of the discrepancy between Bouguer anomalies and isostasy may be related to general westward drift of plates, which creates excess mass in the west. It should be emphasized that the asymmetry of various geophysical parameters with respect to the MAR axis is a reliable fact; however, this topic is not discussed in this paper. The increasing divergence of isostasy and Bouguer anomalies east of–30° W (Fig. 6) is caused by contemporary movements with the vertical component making up the excess mass. In addition to serpentinization, magmatic activity recharged by branches of the African superplume, which has created the volcanic archipelagoes of the Canary and Cape Verde islands, may be the cause of these movements.

DISCUSSION

Our data show that such phenomena as sedimentary cover deformations in abyssal basins, acoustic bleaching of the section, increasing magnetization, and local minima of gravity anomalies are related by a common space and cause-and-effect relationships. The aforementioned phenomena are combined as follows. The heterogeneous lateral movements in basins beyond the MAR are caused by asymmetry of the half-rate of spreading [26] and a different rate from one block to another [37] with contrasting alternation of the cold and hot mantle blocks at a depth of ~500 km. The offsets along the passive parts of transform faults [13] under compression or extension conditions are accompanied by increasing common macrojointing. In the equatorial Atlantic, this is expressed inas variation in the number of troughs controlled by recluse faults in the basins, which exceed in number the reliable transform faults displacing the MAR. This difference is supported by satellite altimetry data [39].

Macrojointing facilitates access of water to the consolidated crust and upper mantle. Conditions favorable for serpentinization of upper-mantle rocks are created during cooling to a temperature lower than 450°C at a certain distance from the MAR [4, 30]. This process is accompanied by crystallization of magnetite, which is an additional component of AMF superposed on linear spreading anomalies. The newly formed fluid migrates upward through the sedimentary sequence along the fault network or via poorly consolidated sediments and gives rise to acoustic bleaching of the section, which has been documented by many seismic records. Since serpentinization is accompanied by an increase in volume, this process is followed by forced folding, which breaks off sediments, forms inclined reflectors, and raises deformed blocks above the common level of the bottom smoothed by sedimentation. A decrease in density and formation of concomitant local gravity minima are consequences of the increase in volume. Thus, the lateral motion of large lithospheric blocks differentiated with depth results in transformation of crustal and mantle rocks with a vertical component of movement and deformation of the sedimentary cover. In areas of plume magmatism, deformation can depend on interaction of the crust and sedimentary cover with locally ascending heated deep-seated material.

According to [20], the statistic distribution of temperature inherent to magnetic phase generation in oceanic peridotite has several peaks near 450°, 320°, and 200°C. This implies that several episodes of serpentinization may occur due to consecutive cooling of the lithosphere as the active zone moves away from the MAR. Analysis of AMF and magnetization (Fig. 4) shows such an undulatory distribution of field maximum coinciding in general with zones of deformation. Probably just this mechanism is responsible for the origination of the so-called zone of abyssal hills [28] localized nearly parallel to the MAR or the zone of marginal dislocations [15], which covers the flanks of the ridge at a distance of 300–350 km from the MAR axis. This is a zone in which Bouguer and isostatic anomalies diverge. Most likely, here we are dealing with the same essence, which in the case of the retained sedimentary cover is accompanied by its deformation in the form of normal faults and inclined reflectors in small sedimentary pockets. As a rule, a sedimentary cover that exceeds the resolution of CSP is extremely rarely deposited within these intervals. Thus, the development of a marginal dislocation zone is caused by cooling of the lithosphere and isostatic compensation of a disturbance that forms in the rift zone.

Deformations are localized above cold blocks at the V_p/V_s slice at a depth of 470 km (Fig. 3). The deformation boundary coincides with surprising accuracy with the zero contour line of theV_p/V_s attribute. It is inexpedient to draw significnat conclusions from this coincidence based on only two intersections; however, it should be noted, because this coincidence opens the way to further search for a correlation of deformation with other geophysical phenomena. Two variants of the relationships between deformations at a relatively shallow depth and geodynamic state of the mantle at a deeper level are suggested:

(1) A shallow-seated layer up to 400 km thick is involved in plate motion in addition to the lithosphere proper; in some localities, cold mantle blocks are the sole of the upper level. The difference in viscosity between the upper and lower layers and friction at the contact between them give rise to deformations at the surface and above cold blocks.

(2) Cold blocks in the upper mantle are a background phenomenon, whereas areas above hot blocks are disturbances arising at plume-related offsets. In this case, the common involvement of the 400-km layer in lateral motion is not an obligatory condition. Instead, we have established intense dynamics only in hot blocks and at their periphery, which determines the interaction and deformations in zones with cold blocks.

At present, it is hardly possible to determine which of the two mechanisms is reliable. The fact that deformations are the result of active influence on the medium in both the vertical and lateral directions speaks in favor of the first solution. Therefore, motion of the layer with elevated friction at its sole in spots of cold blocks appears to have been substantiated. However, plume offsets disturb that state of the mantle where they occur. It cannot be ruled out that both solutions are realized in the nature, competing with each other.

CONCLUSIONS

(1) We have formulated the differences and attributes of deformations in the sedimentary cover of abyssal basins helpful for surveying them. These attributes comprise reflectors in the sedimentary sequence with a slope of $>1^{\circ}$; a constant thickness between reflectors that deviated from the horizontal attitude by more than 1°; faults, piercement structures, structural unconformities; association of structures with acoustic bleaching of sedimentary rocks in form of lenses and gas pipes.

(2) We have established chain of phenomena with common spatial manifestations of heterogeneous lateral movements making up elevated macrojointing above cold mantle blocks at a depth of ~500 km, which deform the crust and sedimentary cover, creating conditions for infiltration of water and serpentinization of the upper-mantle rocks. Superimposed AMF and magnetization anomalies occur, and fluids are released that give rise to acoustic bleaching of the sedimentary sequence. Decompaction of rocks leads to vertical motions and forced folding, which disrupt sediments; inclined reflectors appear; and deformed blocks are lifted above the common bottom level smoothed by sedimentation.

(3) The lithosphere cools with distance from the MAR, creating conditions for several episodes of serpentinization and deformation probably with separation of the zone of abyssal hills and zone of marginal dislocations, which encompass the flanks of ridge, extending for 300–350 km from the axis of the MAR. This zone coincides with the interval characterized by the divergence of Bouguer anomalies and isostasy. The development of the marginal dislocation zone is caused by cooling of the lithosphere and isostatic compensation of the disturbance once formed in rift zone.

(4) Comparison of localization of deformations and cold blocks at the V_p/V_s slice at a depth of 470 km shows that the deformation boundary exactly coincides with the zero contour line of the V_p/V_s attribute.

ACKNOWLEDGMENTS

I thank crews of the R/V *Akademik Nikolai Strakhov* and *Akademik Boris Petrov* for their diligent work under severe conditions, and A.O. Mazarovich and N.P. Chamov for their criticism and comments. This study was carried out under the project "Assessment of Relationships of the Bottom Topography in the Atlantic and Western Arctic Oceans; Sedimentary Cover Deformations, Degassing, and Hazardous Geological Phenomena with the Geodynamic State of the Crust and Upper Mantle" (State Registration no. 01201459183), supported by the Russian Foundation for Basic Research (project nos. 15-05-05888, 14-05-00122) and the Presidium of the Russian Academy of Sciences (Program no. 3: "World Ocean—Multiscale, Multiphase, and Multiparametric").

REFERENCES

1. M. P. Antipov, V. V. Eremeev, and S. M. Zharkov, "Sedimentary cover structure of the central sector of the Atlantic, in the area of the Cape Verde Fracture," in *Sedimentary Cover Structure in the Central Atlantic*, Vol. 449 of *Tr. Geol. Inst. Ross. Akad. Nauk* (Nauka, Moscow, 1990), pp. 95–110.
2. M. E. Artem'ev, T. M. Babaeva, I. E. Voidetskii, V. M. Gordin, and V. O. Mikhailov, *Isostasy and Gravity Field of the Northern Atlantic* (MGK, Moscow, 1987) [in Russian].
3. E. G. Astafurova, A. M. Gorodnitskii, S. V. Luk'yanov, and S. P. Mashchenkov, "Nature of magnetic anomalies and structure of the oceanic crust of the Mid-Atlantic Ridge and the adjacent basins within the limits of the Canaries–Bahamas geotraverse," in *Nature of*

Magnetic Anomalies and Structure of Oceanic Crust, Ed. by A. M. Gorodnitskii (VNIIRO, Moscow, 1996), pp. 171–202.

4. L. V. Dmitriev, B. A. Bazylev, S. A. Silantiev, M. V. Borisov, S. Yu. Sokolov, and A. Bugo, "Hydrogen and methane formation with serpentization of mantle hyperbasites of the ocean and oil generation," Ross. Zh. Nauk Zemle **1**, 511–519 (1999).
5. V. E. Verzhbitskii, Extended Abstract of Candidate (Geol.-Miner.) Sci. Dissertation, (Inst. Oceanol., Ross. Acad. Sci., Moscow, 2000).
6. Yu. N. Voskresenskii, Study of Amplitude Variations in Reflected Seismic Waves For the Purpose of Searching for and Prospecting of Hydrocarbon Fields (Ross. Gos. Univ. Nefti Gaza, Moscow, 2001) [in Russian].
7. O. V. Levchenko, "Strike-slip nature of intraplate deformations in the sedimentary cover of the NE Indian Ocean," in *Geology of Ocean and Seas*, Ed. by A. P. Lisitsin (Inst. Okeanol. Akad. Nauk SSSR, Moscow, 1984), **Vol. 2**, pp. 124–125.
8. O. V. Levchenko, L. R. Merklin, and N. N. Sviridov, "Structure of the sedimentary cover and basement relief in the deep basins of the Atlantic and Indian oceans," in *Geophysical Fields and Bottom Structure of Oceanic Basins*, Ed. by Yu. P. Neprochnov (Nauka, Moscow, 1990), pp. 89–119.
9. O. V. Levchenko, "Central Basin (geophysical fields, crustal structure, and intraplate deformations)," in *Lithosphere of the Indian Ocean Based on the Geophysical Data*, Ed. by A. V. Chekunov and Yu. P. Neprochnov, (Nauk. Dumka, Kiev, 1990), pp. 56–69.
10. A. O. Mazarovich, Yu. I. Morozov, N. N. Turko, "Relief and structure of the sedimentary cover of the Marathon and Mercury fractures (Central Atlantic)," Dokl. Ross. Akad. Nauk, Nauki Zemle **324**, 643–647 (1992).
11. A. O. Mazarovich, "Tectonomagmatic phenomena at flanks of the Arkhangelsky, Doldrams, and Vernadsky transoceanic fractures," Dokl. Ross. Akad. Nauk, Nauki Zemle **332**, 62–65 (1993).
12. A. O. Mazarovich, "Tectonic convergence of transform faults in the near-equatorial Atlantic Ocean," Dokl. Ross. Akad. Nauk, Nauki Zemle **335**, 70–73 (1994).
13. A. O. Mazarovich, *Geologic Structure of the Central Atlantic: Fractures, Volcanic Edifices, and Ocean Floor Deformations* (Nauchn. Mir, Moscow, 2000) [in Russian].
14. A. O. Mazarovich and S. Yu. Sokolov, "Northwest-trending fracture zones in the Central Atlantic Ocean," Geotectonics **3**, 247–254 (2002).
15. Yu. Yu. Odinokov, G. B. Udintsev, and A. F. Beresnev, "Morphological peculiarities of the zone of marginal dislocations of the Mid-atlantic Ridge," Geotektonika, No. 1, 97–115 (1990).
16. V. A. Panaev and S. N. Mitulov, *Seismostratigraphy of the Sedimentary Cover of the Atlantic Ocean* (Nedra, Moscow, 1993) [in Russian].
17. A. I. Pilipenko, "Tectonic deformations of the Brazil Basin," Dokl. Ross. Akad. Nauk, Nauki Zemle **330**, 484–487 (1993).
18. A. I. Pilipenko, "Tectonic lamination of the oceanic crust in deep basins based on seismic data," Geotektonika, No. **1**, 49–61 (1994).
19. A. I. Pilipenko, "Tectonic shortening structures in the western flank of the Mid-Atlantic Ridge (8°–12° S)," Dokl. Ross. Akad. Nauk, Nauki Zemle **340**, 664–666 (1995).
20. K. V. Popov, B. A. Bazylev, and V. P. Shcherbakov, "Temperature range for magnetization of oceanic spinel peridotites," Oceanology **46**, 256–267 (2006).
21. Yu. M. Pushcharovskii, *Tectonics of the Atlantic Ocean with Elements of Nonlinear Gedynamics* (Nauka, Moscow, 1994) [in Russian].
22. Yu. N. Raznitsin and A. I. Pilipenko, "Angola–Brazil geotraverse: Structure and deformations of the oceanic lithosphere," in *Tectonic and Geodynamic Phenomena*, Vol. 505 of *Tr. Geol. Inst. Ross. Akad. Nauk*, Ed. by Yu. M. Pushcharovskii (Nauka, Moscow, 1997), pp. 104–128.
23. Yu. N. Raznitsin, *Tectonic Lamination of the Lithosphere of Young Oceans and Paleobasins*, Vol. 560 of *Tr. Geol. Inst. Ross. Akad. Nauk* (Nauka, Moscow, 2004) [in Russian].
24. *Sedimentary Environments and Facies*, Ed. by H. G. Reading (Blackwell, Oxford, 1986), 2nd ed.
25. S. Yu. Sokolov, "Deformations of sedimentary cover of the equatorial Atlantic and their comparison with the potential fields," in *Tectonics and Geodynamics of the Continental and Oceanic Lithospheres: General and Regional Aspects, Proceedings of the XLVII Meeting on Tectonics* (GEOS, Moscow, 2015), Vol. 2, pp. 172–175.
26. S. Yu. Sokolov, "Shear factor of tectogenesis in the Atlantic Ocean and relationship of this factor to geodynamic state of the upper mantle and intraplate deformations," in *Tectonics, Geodynamics, and Ore Genesisof Folded Zones and Platforms, Proceedings of the XLVIII Meeting on Tectonics* (GEOS, Moscow, 2016), Vol. 2, pp. 178–184.
27. *Physical Properties of Rocks and Mineral Resources (Petrophysics): A Reference Book for Geophysicists*, Ed. by N. B. Dortman (Nedra, Moscow, 1984), 2nd ed. [in Russian].
28. B. C. Heezen, M. Tharp, and M. Ewing, *The Floors of the Oceans: Part I, the North Atlantic*, Vol. 65 of *Geol. Soc. Am., Spec. Pap.* (1959).
29. T. W. Becker, L. Boschi, "A comparison of tomographic and geodynamic mantle models," Geochem. Geophys. Geosyst. **3**, 1–48 (2002). doi 10.129/2001GC000168
30. J. L. Charlou, Y. Fouquet, H. Bougault, J. P. Donval, J. Etoubleau, P. Jean-Baptiste, A. Dapoigny, P. Appriou, and P. Rona, "Intense CH_4 plumes generated by serpentinization of ultramafic rocks at the intersection of the 15°20' N fracture zone and the Mid-Atlantic Ridge," Geochim. Cosmochim. Acta **62**, 2323–2333 (1998).
31. V. N. Efimov, A. V. Koltsova, A. F. Beresnev, V. M. Golod, S. Yu. Sokolov, and M. V. Zakharov, "The structure of sedimentary cover from single-channel profiling data," in *Equatorial Segment of the Mid-Atlantic Ridge: IOC Technical series No. 46, Initial Results of the Geological and Geophysical Investigations under the EQUARIDGE Program, Cruises of R/V 'Akademik Nikolaj Strakhov' in 1987, 1990, 1991*, Ed. by G. B. Udintsev (UNESCO, Paris, 1996), pp. 19–24.

32. K. O. Emery and E. Uchupi, *The Geology of the Atlantic Ocean* (Springer, New York, 1984).
33. *Equatorial Segment of the Mid-Atlantic Ridge: IOC Technical series No. 46, Initial Results of the Geological and Geophysical Investigations under the EQUARIDGE Program, Cruises of R/V 'Akademik Nikolaj Strakhov' in 1987, 1990, 1991*, Ed. by G. B. Udintsev (UNESCO, Paris, 1996). Text: 128 p. Atlas: 32 p.
34. S. P. Grand, R. D. van der Hilst, and S. Widiyantoro, "Global seismic Tomography: A snapshot of convection in the Earth," GSA Today **7** (4), 1–7 (1997).
35. D. E. Hayes, A. C. Pimm, J. P. Beckmann, W. E. Benson, W. H. Berger, P. H. Roth, P. R. Supko, and U. Von Rad, "Site 138," in Vol. XIV of *Initial Reports of the Deep Sea Drilling Project* (1970), pp. 135–155.
36. S. Maus, U. Barckhausen, H. Berkenbosch, N. Bournas, J. Brozena, V. Childers, F. Dostaler, J. D. Fairhead, C. Finn, R. R. B. von Frese, C. Gaina, S. Golynsky, R. Kucks, H. Luhr, P. Milligan, et al., "EMAG2: A 2-arc-minute resolution Earth Magnetic Anomaly Grid compiled from satellite, airborne and marine magnetic measurements," Geochem. Geophys. Geosyst. **10**, Pap. No. Q08005 (2009). doi 10.1029/2009GC002471
37. R. D. Muller, M. Sdrolias, C. Gaina, and W. R. Roest, "Age, spreading rates, and spreading asymmetry of the world's ocean crust," Geochem. Geophys. Geosyst. **9**, Pap. No. Q04006 (2008). doi 10.1029/2007GC001743
38. G. Peter and G. K. Westbrook, "Tectonics of southwestern north Atlantic and Barbados ridge complex," AAPG Bull. **60**, 1078–1106 (1976).
39. D. T. Sandwell and W. H. F. Smith, "Global marine gravity from retracked Geosat and ERS-1 altimetry: Ridge segmentation versus spreading rate," J. Geophys. Res.: Solid Earth **114**, 1–18 (2009). doi 10.1029/2008JB006008
40. R. C. Searle, "GLORIA investigations of oceanic fracture zones: Comparative study of the transform fault zone," J. Geol. Soc. (London, U.K.) **143**, 743–756 (1986).
41. T. H. Van Andel, R. P. Von Herzen, J. D. Phillips, "The Vema fracture zone and the tectonics of transverse shear zones in oceanic crustal plates," Mar. Geophys. Res. **1**, 261–283 (1971).
42. R. D. Van der Hilst, S. Widiyantoro, and E. R. Engdahl, "Evidence of deep mantle circulation from global tomography," Nature **386**, 578–584 (1997).
43. GEBCO 30" Bathymetry Grid, Version 20141103, 2014. http://www.gebco.net.
44. GEODAS, Marine Trackline Geophysical Data, 2010. http://www.ngdc.noaa.gov/mgg/geodas/trackline.html.

Reviewer: Yu.A. Volozh
Translated by V. Popov

SPELL: OK